






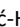




# Analysis of Antitumor Potential of Xanthene Compounds in Lymphoma Cells

 Esma Bilajac,<sup>1</sup>  Una Glamočlija,<sup>2,3,4,\*</sup>  Amar Osmanović,<sup>2</sup>  Lejla Mahmutović,<sup>1</sup>  Abas Sezer,<sup>1</sup>  Sunčica Roca,<sup>5</sup>  
 Selma Špirtović-Halilović,<sup>2</sup>  Mirsada Salihović,<sup>2</sup>  Altijana Hromić-Jahjefendić,<sup>1</sup>  Elma Veljović<sup>2</sup>

<sup>1</sup> Department of Genetics and Bioengineering, Faculty of Engineering and Natural Sciences, International University of Sarajevo, Hrasnička cesta 15, 71000 Sarajevo, Bosnia and Herzegovina

<sup>2</sup> University of Sarajevo - Faculty of Pharmacy, Zmaja od Bosne 8, 71000 Sarajevo, Bosnia and Herzegovina

<sup>3</sup> School of Medicine, University of Mostar, Zrinskog Frankopana 34, 88000 Mostar, Bosnia and Herzegovina

<sup>4</sup> Scientific-Research Unit, Bosnalijek JSC, Jukićeva 53, 71000 Sarajevo, Bosnia and Herzegovina

<sup>5</sup> NMR Centre, Ruđer Bošković Institute, Bijenička cesta 54, 10000 Zagreb, Croatia

\* Corresponding author's e-mail address: una.glamočlija@ffsa.unsa.ba

RECEIVED: June 22, 2023 \* REVISED: July 27, 2023 \* ACCEPTED: July 29, 2023

**Abstract:** Antitumor activity of two newly and sixteen previously synthesized 9-arylsubstituted 2,6,7-trihydroxyxanthene-3-ones on diffuse large B-cell lymphoma cells were analyzed in this study. Xanthene derivatives are characterized with numerous therapeutic applications, including anticancer, antioxidant, anti-inflammatory and other activities. *In silico* molecular docking analysis suggests significant binding affinities of certain compounds toward Akt and NF- $\kappa$ B proteins as two major players of cell proliferation and differentiation. Results of WST-8 assay indicate mild or no activity of xanthene compounds on cell viability of HBL-1 and DHL-4 cell lines belonging to ABC and GCB DLBCL subtypes, respectively. Western blotting showed stimulatory activity of certain compounds, with increased expression of Akt in HBL-1 and DHL-4 cells. Our results provide an insight into activation of compensatory Akt mechanism in DLBCL models that could be an important step for further approaches in application of dual inhibitors for cancer treatment to achieve greater therapeutic effectiveness and drug resistance escape.

**Keywords:** xanthene-3-ones, cancer, diffuse large B-cell lymphoma, compensatory mechanisms, molecular docking analysis.

## INTRODUCTION

CANCER is a major health problem worldwide, with approximately 19.3 million of newly diagnosed cases and 10 million of cancer related deaths in 2020.<sup>[1]</sup> Cancer development is associated with different genetic and epigenetic alterations, allowing cells to proliferate and grow uncontrollably. Oncogenic mutations result in deregulation of numerous signaling pathways, such as phosphoinositide 3-kinase (PI3K) and receptor tyrosine kinase pathways and other. Mutations in transcription factors, such as nuclear factor kappa B (NF- $\kappa$ B), can also be detected in many cancer types.<sup>[2]</sup>

PI3K activation has an important role in cancer progression, regulating tumor growth, survival, and proliferation. Stimulation of PI3K by various extracellular signals leads to activation of Akt serine/threonine kinase,

promoting cancer cell growth.<sup>[3–6]</sup> NF- $\kappa$ B signaling regulates numerous intracellular processes, including immune response, inflammation, cell survival, proliferation and differentiation. NF- $\kappa$ B belongs to a family of NF- $\kappa$ B transcription factors that translocate into the nucleus, initiating transcription of plentiful genes involved in distinctive cellular functions.<sup>[7]</sup>

Diffuse large B-cell lymphoma (DLBCL) is the most common non-Hodgkin's lymphoma (NHL), with 30–40 % of total number of newly diagnosed B-cell NHL cases in multiple geographical regions.<sup>[8–10]</sup> DLBCL represents heterogeneous group of neoplasms that differ at biological, molecular, pathological and clinical level.<sup>[8,11–13]</sup> DLBCL is classified into two distinct molecular subgroups, activated B-cell (ABC) (40–50 %) and germinal center B-cell (GCB) (50–60 %) DLBCL.<sup>[14]</sup> The main hallmark of ABC DLBCL is constitutive activation of NF- $\kappa$ B signaling that promotes cell

differentiation and proliferation,<sup>[15]</sup> whereas GCB DLBCL cells depend on constitutive activation of PI3K signaling pathway, resulting in uncontrolled cancer cell survival and growth.<sup>[16,17]</sup>

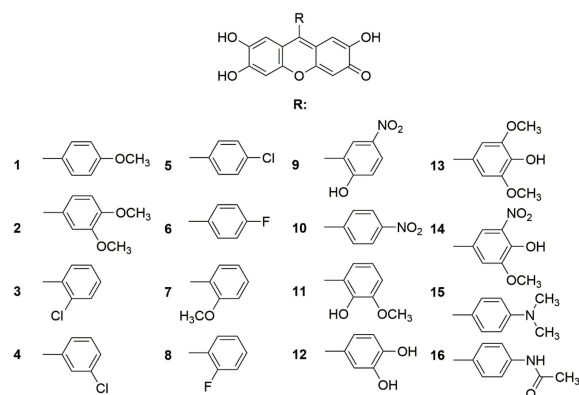
Considering the urge for development of novel and highly effective therapies for DLBCL, we have synthesized and evaluated the potential antitumor effect of 9-arylsubstituted 2,6,7-trihydroxyxanthene-3-ones. Xanthenes, a biologically active tricyclic compounds with dibenzopyran nucleus, are characterized with broad range of therapeutic applications that include antibacterial, antiviral, anticancer, antioxidant, antimicrobial, anti-inflammatory, immunomodulatory and enzyme inhibitory activities.<sup>[18–24]</sup>

We have previously reported significant antitumor activity of various xanthene derivatives in hepatocellular, cervical adenocarcinoma, metastatic colon carcinoma and non-small cell lung cancer cells.<sup>[18,19]</sup> Other research groups reported promising antitumor activity of xanthene derivatives in breast, prostate, oral cavity cancer, as well as promyelocytic leukemia cells.<sup>[20,25,26]</sup> Currently, a photosensitizing xanthene dye Rose Bengal disodium (PV-10) is included in clinical trials for patients with metastatic melanoma, liver and recurrent breast cancer patients with minimum cytotoxicity on fibroblast models.<sup>[20–27]</sup> The aim of this study was to synthesize novel xanthene derivatives and evaluate their activity in ABC and GCB DLBCL cells.

## EXPERIMENTAL

### Instrumentation

Melting points of the compounds were determined with BÜCHI Melting Point B-545 and are presented uncorrected. The <sup>1</sup>H and <sup>13</sup>C nuclear magnetic resonance (NMR) spectra were recorded at 600 and 150 MHz, respectively, in DMSO-d<sub>6</sub> at 25 °C using NMR spectrometer Bruker AV600, with tetramethylsilane (TMS) as internal reference (see



**Figure 1.** Structures of previously synthesized xanthene derivatives.<sup>[18,19]</sup>

*Supplementary Material*). Chemical shifts ( $\delta$ ) are reported in ppm and coupling constants ( $J$ ) in Hz. Elemental analyses of synthesized compounds were recorded by Vario EL III C,H,N,S/O Elemental Analyzer, Elementar Analysensysteme GmbH, Hanau-Germany (see *Supplementary Material*). The analysis of mass spectra was performed on an LC-MS/MS apparatus (Agilent Technologies, Waldbronn, Germany), which consists of an HPLC 1200 device with a binary pump, a degasser and an autosampler. The HPLC was connected to a 6420 mass spectrometer with triple quadrupole and ESI ionization in negative mode. The samples were dissolved in methanol to a concentration of about 100  $\mu\text{g mL}^{-1}$  and injected into the system with 50 % methanol elution.

### Previously and Newly Synthesized Xanthene Derivatives

In our previous work we synthesized and confirmed structure of sixteen 2,6,7-trihydroxy-9-aryl-3H-xanthene-3-one derivatives (Figure 1, Table 1).<sup>[28,29]</sup> New xanthene-3-one derivatives were synthesized from 1,2,4-triacetoxybenzene (5 g, 20 mmol) and different aromatic aldehydes (10 mmol)

**Table 1.** List of chemical names of previously synthesized xanthene-3-one derivatives.

Name	Compound
2,6,7-trihydroxy-9-(4-methoxyphenyl)-3H-xanthene-3-one	1
9-(3,4-dimethoxyphenyl)-2,6,7-trihydroxy-3H-xanthene-3-one	2
9-(2-chlorophenyl)-2,6,7-trihydroxy-3H-xanthene-3-one	3
9-(3-chlorophenyl)-2,6,7-trihydroxy-3H-xanthene-3-one	4
9-(4-chlorophenyl)-2,6,7-trihydroxy-3H-xanthene-3-one	5
9-(4-fluorophenyl)-2,6,7-trihydroxy-3H-xanthene-3-one	6
2,6,7-trihydroxy-9-(2-methoxyphenyl)-3H-xanthene-3-one	7
9-(2-fluorophenyl)-2,6,7-trihydroxy-3H-xanthene-3-one	8
2,6,7-trihydroxy-9-(2-hydroxy-5-nitrophenyl)-3H-xanthene-3-one	9
2,6,7-trihydroxy-9-(4-nitrophenyl)-3H-xanthene-3-one	10
2,6,7-trihydroxy-9-(2-hydroxy-3-methoxyphenyl)-3H-xanthene-3-one	11
9-(3,4-dihydroxyphenyl)-2,6,7-trihydroxy-3H-xanthene-3-one	12
2,6,7-trihydroxy-9-(4-hydroxy-3,5-dimethoxyphenyl)-3H-xanthene-3-one	13
2,6,7-trihydroxy-9-(4-hydroxy-3-methoxy-5-nitrophenyl)-3H-xanthene-3-one	14
9-(4-(dimethylamino)phenyl)-2,6,7-trihydroxy-3H-xanthene-3-one	15
9-(4-acetamidophenyl)-2,6,7-trihydroxy-3H-xanthene-3-one	16

under acidic alcoholic conditions (75 mL 50 % ethanol, 3 mL conc. sulfuric acid). After a two-fold Friedel-Crafts alkylation intermediate **A** was obtained. For accomplishing the transformation, a single trihydroxy benzene moiety of **A** had to be oxidized using potassium peroxodisulphate (2.7 g, 10 mmol) to the corresponding *p*-benzoquinone. To avoid decomposition of potassium peroxodisulphate, the reaction of oxidation occurred at 80 °C. Benzoquinone intermediate (**B**) subsequently underwent a cyclocondensation reaction to the xanthenone fragment. To remove potassium peroxodisulphate after completed oxidation, refluxed suspension was poured onto ice water and filtered. The residue was dried under vacuum at 60 °C. Structure and analytical data of the compounds **17** and **18** are presented in this paper in the Results and Discussion part (Figure 2).

### Molecular Docking Analysis

The molecular docking study was set up in YASARA Structure 19.12.14 software<sup>[30,31]</sup> and performed using AutoDock 4.2.<sup>[32]</sup> The crystal structures of I-Kappa-B-Alpha/NF-Kappa-B (PDB ID: 1NFI), NF-kB p52/RelB/DNA complex (PDB ID: 3DO7) and murine PI3K p110 delta (PDB ID: 5NGB) were downloaded from RCSB Protein Data Bank (<https://www.rcsb.org/>) and used as target molecules. The structures of protein targets were prepared by removing water molecules, adding polar hydrogen atoms and optimizing in the AMBER03 force field.<sup>[33]</sup> The 3D structures of the xanthene molecules were prepared and geometries were optimized by the MM2 force field<sup>[34,35]</sup> using PerkinElmer Chem3D Ultra 16.0.1.4. software. Molecular docking analyses were performed using either the blind docking method (for targets 1NFI and 3DO7) or setting up the search area box around a specific binding pocket (for the 5NGB target). The Lamarckian genetic algorithm was employed with the following parameters: 10 docking runs with a maximum of 15,000,000 energy evaluations and 27,000 generations for each run, with a grid point spacing of 0.375 Å, providing this way the lowest energy docked poses. YASARA Structure 19.12.14 software was used for visualization and image creation.

### Cell Culture and Substance Preparation

HBL-1 and DHL-4 cell lines were cultured in Roswell Park Memorial Institute (RPMI)-1640 basal medium (Sigma Aldrich, USA) supplemented with 10 % Fetal Bovine Serum (FBS), 100 U mL<sup>-1</sup> penicillin, 100 U mL<sup>-1</sup> streptomycin, 10 mM HEPES, 1 mM sodium pyruvate and 1 % of non-essential amino acid  $\alpha$ -glutamine (Sigma Aldrich, USA). DHL-4 is a B-cell lymphoma cell line assigned to GCB lymphoma subtype and B-cell receptor DLBCL.<sup>[46]</sup> HBL-1 is a diffuse large B-cell lymphoma carrying 14q32 translocation and it is assigned to ABC lymphoma subtype and B-cell receptor DLBCL.<sup>[46]</sup>

Cell cultures were grown in suspension and maintained at optimal conditions in humidified atmosphere (95 %), 5 % CO<sub>2</sub> at 37 °C. The compounds were dissolved in 100 % dimethyl sulfoxide (DMSO) (Sigma-Aldrich, UK) as a stock solution of 100 mM concentration and further diluted in 1× phosphate buffered saline (PBS) (Fisher Bioreagents, USA).

### Cell Viability Assay

Cell viability was determined by WST-8 assay (Bimake, USA). Cells were plated in triplicates in a 96-well plate at optimum seeding density of  $2.5 \times 10^4$  cells/well and treated with different compounds' concentrations for 48 hours. The highest percentage of DMSO in wells treated with compounds was 0.05 %. The same percentage of DMSO was used as negative control. After incubation, cell viability assay was performed according to the manufacturer's protocol.

### Western Blot Analysis

For Western blot analysis, cells were seeded in a 6-well plate at a seeding density of  $1 \times 10^6$  cells/well and treated with compounds 9, 10 and 14 for 48 hours, while cells treated with 0.05 % DMSO were used as a negative control. Cells were lysed in ice-cold RIPA buffer supplemented with protease and phosphatase inhibitors (Sigma-Aldrich, UK). All samples were separated by 12 % SDS-polyacrylamide gel electrophoresis (SDS-PAGE) and transferred onto a polyvinylidene difluoride (PVDF) membrane (Merck Millipore, Germany). The membrane was blocked with 5 % BSA in Tris-buffered saline supplemented with 0.1 % Tween-20 buffer (Sigma-Aldrich, UK). Western blot analyses were performed using primary antibodies against phospho-NF- $\kappa$ B p65 (Ser536) (93H1) Rabbit mAb #3033, phospho-Akt (Ser473) (D9E) XP<sup>®</sup> Rabbit mAb #4060, and PI3 Kinase p110  $\delta$  (D1Q7R) Rabbit mAb #34050. For loading control  $\beta$ -Actin (8H10D10) Mouse mAb #3700 primary antibody was used. Secondary antibodies anti-rabbit IgG, HRP-linked Antibody #7074 and anti-mouse IgG, HRP-linked Antibody #7076 were used (Cell Signaling Technology, USA). The signals were detected using Amersham<sup>™</sup> ECL Prime Western Blotting Detection Reagent (GE Healthcare Life Sciences, UK). Protein bands were visualized by Molecular Imager ChemiDoc<sup>™</sup> XRS+ Imaging System (Bio-Rad, USA) and analyzed by Image Lab software (v.6.0).

### Statistical Analysis

GraphPad PRISM software, version 8.3 was used for statistical analysis. The results of different experiments were represented as means  $\pm$  standard deviation (SD) of three to four independent experiments. Normal distribution of variances was tested by D'Agostino-Pearson normality test.

Shapiro-Wilk test was used where normality test indicated normal distribution of variances ( $p > 0.05$ ), whereas Kolmogorov-Smirnov test was used otherwise. One-way ANOVA Dunnett's multiple comparison analysis was used for statistical evaluation.  $p < 0.05$  was considered as level of statistical significance with the next levels presented through the text: \* $p < 0.05$ , \*\* $p < 0.01$ , \*\*\* $p < 0.001$ , \*\*\*\* $p < 0.0001$ , ns – not significant.

## RESULTS AND DISCUSSION

### Chemistry

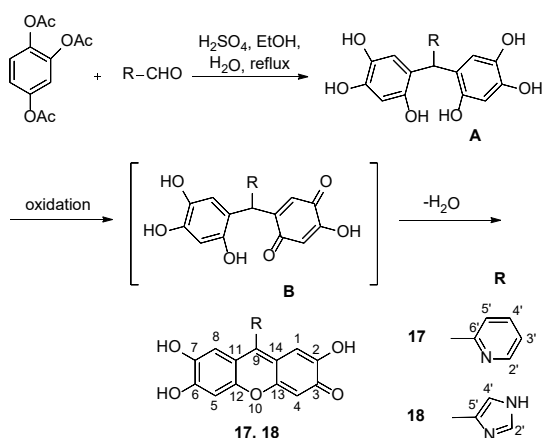
The synthetic pathway is shown in Figure 2, adapted from References 28 and 29.

#### 2,6,7-TRIHYDROXY-9-(PYRIDIN-2-YL)-3H-XANTHENE-3-ONE (COMPOUND 17)

Yield: 92 %; m.p. 165–168 °C;  $^1\text{H}$  NMR (600 MHz, DMSO- $d_6$ ):  $\delta$  8.91 (1H, dd,  $J = 5.37, 1.72$  Hz, H-6'), 8.15 (1H, td,  $J = 7.66, 1.74$  Hz, H-4'), 7.71–7.67 (2H, m, H-3'/5'), 6.95 (2H, s, H-4/5), 6.49 (2H, s, H-1/8), 9.84 and 5.15 (br s, OH) ppm.  $^{13}\text{C}$  NMR (150 MHz, DMSO- $d_6$ ):  $\delta$  163.5 (2C, C-11/12), 152.7 (2C, C-2/7 or C-3/6), 152.2 (1C, C-2'), 150.1 (1C, C-6'), 147.7 (2C, C-2/7 or C-3/6), 146.4 (1C, C-9), 137.4 (1C, C-4'), 125.6 (1C, C-3'), 124.4 (1C, C-5'), 115.3 (2C, C-10/13), 107.0 (2C, C-1/8), 102.4 (2C, C-4/5) ppm; ESI-MS ( $m/z$ ): 320.00 (M-H) $^-$ ; Anal. calc. for  $\text{C}_{18}\text{H}_{11}\text{NO}_5$  (321.06): C 67.29, H 3.45, N 4.36, found: C 67.21, H 3.48, N 4.32.

#### 2,6,7-TRIHYDROXY-9-(1H-IMIDAZOL-4-YL)-3H-XANTHENE-3-ONE (COMPOUND 18)

Yield: 72.3 %; m.p. 212–214 °C;  $^1\text{H}$  NMR (600 MHz, DMSO- $d_6$ ):  $\delta$  9.07 (1H, s, H-2'), 8.11 (1H, s, H-5'), 6.97 (2H, s, H-1/8), 6.88 (2H, s, H-4/5), 9.85 and 4.47 (br s, OH) ppm.  $^{13}\text{C}$  NMR (150 MHz, DMSO- $d_6$ ):  $\delta$  151.8 (2C, C-2/7 or C-3/6), 147.9



**Figure 2.** Synthetic scheme for xanthene-3-one derivatives and structure of the two newly synthesized compounds.

(2C, C-2/7 or C-3/6), 137.0 (1C, C-2'), 126.3 (1C, C-4'), 122.1 (1C, C-5'), 115.7 (2C, C-10/13), 107.2 (2C, C-1/8), 102.5 (2C, C-4/5) ppm; ESI-MS ( $m/z$ ): 309.00 (M-H) $^-$ ; Anal. calc. for  $\text{C}_{16}\text{H}_{10}\text{N}_2\text{O}_5$  (310.06): C 61.94, H 3.25, N 9.03, found: C 61.97, H 3.19, N 9.12.

### Molecular docking analysis

Molecular docking analysis on xanthene derivatives showed significant binding affinities toward certain protein targets (Table 2, Figure 3). The results showed that compound **10** and compound **14** formed the most significant complexes with unphosphorylated protein kinase B/Akt (PDB ID: 1GZO) and PI3K p110 $\delta$  (PDB ID: 5NGB) with binding

**Table 2.** Molecular docking parameters for xanthene derivatives with target proteins.

Comp.	Binding energy / kcal mol $^{-1}$	Dissociation constant / $\mu\text{M}$	Contacting amino acid residues (H-bonds)
Protein kinase B unphosphorylated (PDB ID: 1GZO)			
<b>14</b>	-9.45	0.118	Tyr 316
<b>18</b>	-9.04	0.235	Ile 276, Leu 278
<b>10</b>	-8.73	0.396	Lys 156, Glu 279
<b>9</b>	-7.66	2.450	Arg 208, Lys 290
NF- $\kappa$ B/p52/RelB/DNA complex (PDB ID: 3D07)			
<b>9</b>	-11.20	0.0056	Arg 117, Lys 273, Thr 276, Lys 283, Lys 305
<b>18</b>	-10.93	0.010	Arg 241, Tyr 294
<b>12</b>	-10.90	0.010	Arg 241, Tyr 294
<b>11</b>	-10.26	0.030	Arg 117, Lys 273, Lys 283, Lys 305
<b>2</b>	-9.70	0.077	Gly 115, Arg 117, Arg 125, Ile 207
<b>13</b>	-9.57	0.097	Tyr 294
<b>16</b>	-9.32	0.147	-
<b>10</b>	-9.30	0.151	Ala 104
<b>14</b>	-8.74	0.392	Lys 210, Asn 242
<b>17</b>	-8.73	0.411	Arg 117, Leu 203, Ile 205, Lys 273
<b>15</b>	-8.71	0.525	Leu 95, His 105
PI3K p110 delta (PDB ID: 5NGB)			
<b>10</b>	-10.56	0.018	Lys 779, Tyr 813, Glu 826, Val 828
<b>14</b>	-10.31	0.028	Lys 779, Asp 787
<b>12</b>	-10.03	0.045	Asp 787, Glu 826, Val 828, Asp 911
<b>16</b>	-9.44	0.119	Ser 754, Lys 779, Asp 787
<b>11</b>	-9.19	0.184	Lys 779, Asp 787
<b>9</b>	-9.08	0.221	Lys 779, Val 828
<b>13</b>	-9.05	0.230	Asp 787, Val 828

values lower than  $-8.5$  kcal mol $^{-1}$ . Compound **9** formed strong complexes with NF- $\kappa$ B/p52/RelB/DNA complex (PDB ID: 3DO7), with dissociation constant of  $0.0056$   $\mu$ M.

Besides hydrogen bonds (H-bonds), other types of bonds such as hydrophobic,  $\pi$ - $\pi$  and cation- $\pi$  bonds were observed upon binding of derivatives to the target proteins. Figure 3 represents binding modes of compounds **9**, **10** and **14** with unphosphorylated protein kinase B (PDB ID: 1GZO), NF- $\kappa$ B/p52/RelB/DNA complex (PDB ID: 3DO7), and PI3K p110 delta (PDB ID: 5NGB) assessed by molecular docking study.

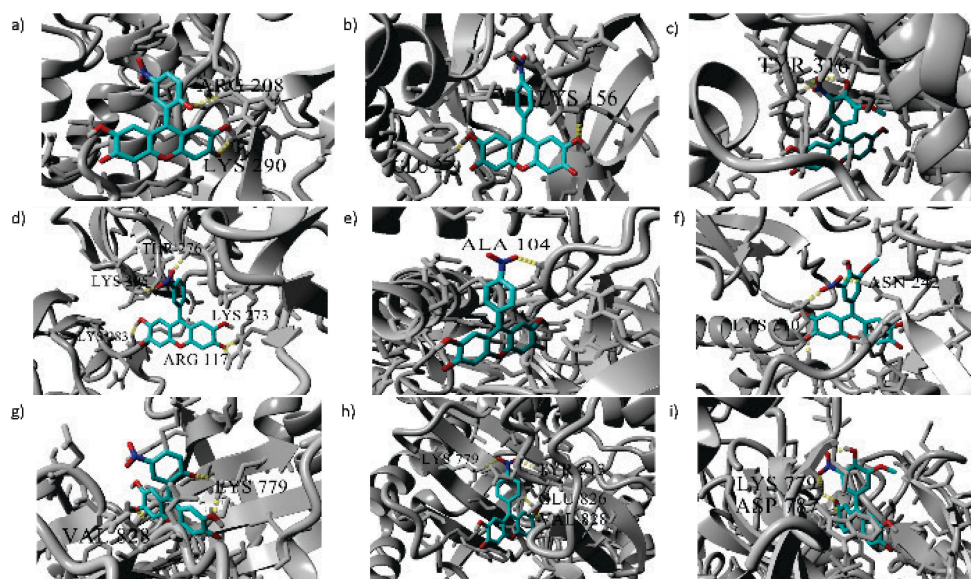
### Compounds' Effects on DLBCL Cell Metabolic Activity

Using WST-8 assay, we evaluated the effect of xanthene derivatives on metabolic activity of ABC (HBL-1) and GCB (DHL-4) DLBCL cells. Derivatives have shown either mild or no inhibitory activity (Figure 4 and 5). Mild inhibitory activity was denoted where percentage of viable cells ranged between 60–80 % at 50  $\mu$ M concentration of compound, otherwise the compounds were denoted to have no inhibitory activity (cell viability remained above 80 % at the same concentration). Importantly, the cytotoxic effects of certain compounds varied between the two DLBCL subtypes, suggesting different mechanisms of action. In ABC DLBCL HBL-1 cells, compounds **1**, **2**, **3**, **4**, **5**, **6**, **7**, **8**, and **15** exhibited mild inhibitory activity. Treatment with compounds **9**, **10**, **11**, **12**, **13**, **14**, **16**, **17** and **18** showed no inhibitory activity in HBL-1 cell line (Figure 4a, b). In contrast to HBL-1 cell line, compounds **1**, **2**, **3**, **4**, **6**, **7**, and **8** showed no inhibitory

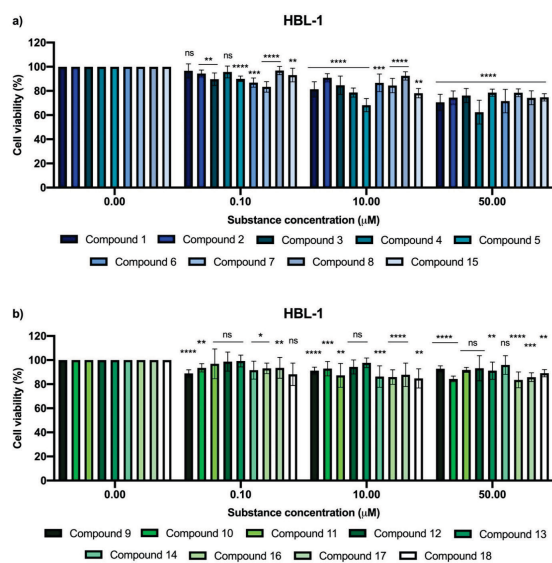
activity in DHL-4 cells, whose inhibitory effect on HBL-1 cells was mild. DHL-4 cells showed mild inhibitory response to the treatment with compounds **10**, **11**, **12**, **14**, **16**, and **17**, while ABC DLBCL cells showed no significant sensitivity to the treatment with mentioned compounds. Compounds **5** and **15** had mild inhibitory activity in both cell lines. Compounds **9**, **13**, and **18** did not have inhibitory activity in both, DHL-4 and HBL-1 cell lines (Figure 4 and 5).

Our data suggest different responses of HBL-1 and DHL-4 cells toward treatment with xanthene derivatives. The treatment with the compounds characterized with mild inhibitory activity induced significant decrease of cell viability ( $p < 0.0001$ ) in both cell lines at the highest treatment concentration (50  $\mu$ M). The inhibitory concentration 50 ( $IC_{50}$ ) was  $> 50.00$   $\mu$ M for all compounds in both cell lines.

Xanthene derivatives with central oxygen-containing heterocyclic structure fused to two more cyclic structures possess wide range of biological activities. The structure-activity relationship (SAR) of xanthenes suggests that these derivatives induce anti-proliferative properties in cancer models in respect to distinct moieties.<sup>[36,37]</sup> In one study, antitumor activity and SAR of several *N*-substituted 14-aryl-14*H* dibenzo[*a,j*]xanthene-3,11-dicarboxamides was evaluated in acute promyelocytic leukemia and hepatoma cancer cells. SAR analysis revealed that numerous parameters affect the compounds' activity, including side chain positions, substituent size and other. Accordingly, carboxamide substituent at C-3 and C-11 positions induced stronger inhibitory activity, while the small size of the positioned group on nitrogen atom of the carboxamide side chain



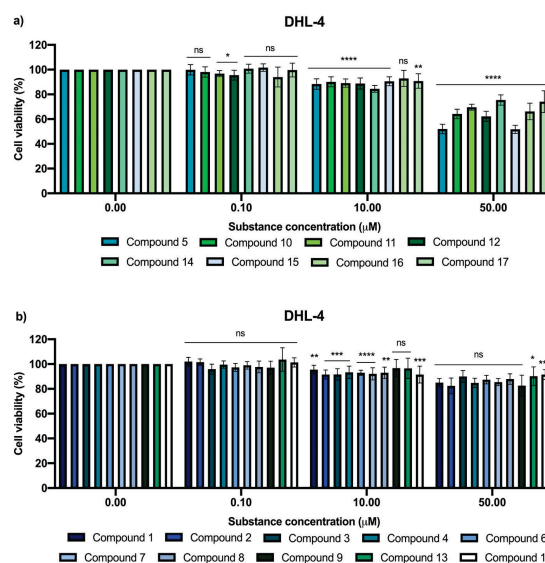
**Figure 3.** Binding modes of compounds **9**, **10** and **14** at the active site of (a–c) unphosphorylated protein kinase B (PDB ID: 1GZO), (d–f) NF- $\kappa$ B/p52/RelB/DNA complex (PDB ID: 3DO7), and (g–i) PI3K p110 delta (PDB ID: 5NGB) assessed by molecular docking study.



**Figure 4.** Effect of compounds on cell viability after 48 hour incubation in HBL-1 cell line showing (a) mild and (b) no inhibitory activity. Graphs represent the average of triplicates from three independent experiments with standard deviations indicated for each concentration. Cell viability is represented as a percentage compared to 0.05 % DMSO control.  $p < 0.05$  was considered as level of statistical significance with the next levels: \* $p < 0.05$ , \*\* $p < 0.01$ , \*\*\* $p < 0.001$ , \*\*\*\* $p < 0.0001$ .

resulted in greater cytotoxicity rates of the compounds. Addition of halogen substituents at the *para* position of the 14-phenyl ring resulted in lower  $IC_{50}$  values and increased inhibitory activity in comparison to other substituents positioned differently.<sup>[37,38]</sup> Moreover, position of chlorine group in other synthesized derivatives, such as benzyloxyphenylmethylaminophenol also have an important role in induction of inhibitory activities. In HepG2 hepatocellular carcinoma cells, compound with chloro group positioned at C-3 in the ring showed very strong cytotoxicity in cancer cells ( $IC_{50} = 1.38 \mu\text{M}$ ), while the compound with chlorine at position C-5 induced less inhibitory activity ( $IC_{50} = 26.68 \mu\text{M}$ ), with reduced inhibitory activity toward STAT3 expression.<sup>[39]</sup>

In our study, xanthene derivatives mainly showed opposing effects in DLBCL cells belonging to two distinct subtypes, possibly as a result of different intracellular mechanisms of action. However, our results showed that compound **5** (4-chlorophenyl) induced mild inhibitory activity in both DLBCL models. This can be linked to the position of the chlorine substituent at C-4 position as compounds **3** and **4** with chlorine atom at C-2 and C-3, respectively, induced no inhibitory activity in DHL-4 cells. In addition, our data suggest that HBL-1 cells were more sensitive to the treatment with xanthene derivatives bearing methoxy



**Figure 5.** Effect of compounds on cell viability after 48 hour incubation in DHL-4 cell line showing (a) mild and (b) no inhibitory activity. Graphs represent the average of triplicates from three independent experiments with standard deviations indicated for each concentration. Cell viability is represented as a percentage compared to 0.05% DMSO control.  $p < 0.05$  was considered as level of statistical significance with the next levels presented: \* $p < 0.05$ , \*\* $p < 0.01$ , \*\*\* $p < 0.001$ , \*\*\*\* $p < 0.0001$ .

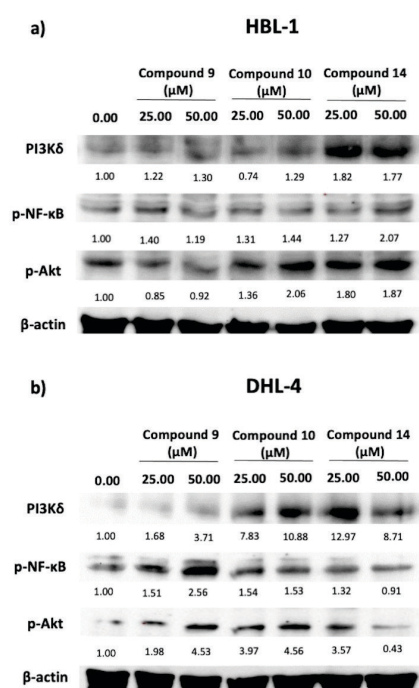
( $\text{OCH}_3$ ) and fluorine substituent. This could possibly be linked to the expression of distinct molecular signaling pathways in ABC DLBCL cells where the mentioned compounds bind to specific targets inside of the cell.

### Evaluation of Compounds' Protein Targets in HBL-1 and DHL-4 Cell Lines

Based on the *in silico* analysis results, we studied the effects of compounds **9**, **10** and **14** on the expression of different protein targets that regulate cell survival, proliferation and differentiation of DLBCL cells. The cells were treated with two concentrations of compounds (25 and 50  $\mu\text{M}$ ) for 48 hours (Figure 6).

The expression levels of phosphorylated NF- $\kappa\text{B}$  protein, as one of the major drivers of ABC DLBCL pathogenesis leading to uncontrolled cell differentiation and proliferation, were increased in HBL-1 cells following treatment with compounds **9**, **10**, and **14**.

The most prominent effect was observed after the treatment with 50  $\mu\text{M}$  concentration of compound **14**, where the expression of p-NF- $\kappa\text{B}$  increased in average for two-fold in comparison to the control group. In the same cells, the expression levels of PI3K $\delta$  p110 protein that is involved in cell growth and division also increased after the



**Figure 6.** Evaluation of protein expression after treatment with compounds **9**, **10** and **14** for 48 hours in HBL-1 and DHL-4 cells. Numbers below the bands represent a net image fold difference in the band intensity compared to the control and normalization against  $\beta$ -actin.

treatment with selected compounds. The expression of PI3K $\delta$  protein was the strongest after treatment with compound **14**. Treatment of HBL-1 cell line with compound **9** resulted in similar expression of activated Akt as a major player of PI3K/Akt/mTOR signaling compared to the control. However, compounds **10** and **14** stimulated the expression of p-Akt protein in HBL-1 cells, with greater effect on its expression after the treatment with 50  $\mu$ M concentration of compound **10** (Figure 6).

In DHL-4 cells, we observed increased expression of p-NF- $\kappa$ B following treatment with compounds **9** and **10**, where the expression of target protein increased more than two-fold compared to the control. However, compound **14** resulted in similar expression of p-NF- $\kappa$ B at 50  $\mu$ M treatment concentration compared to control. Compounds **9**, **10** and **14** induced overexpression of PI3K $\delta$  protein, with the greatest stimulatory effect after compound **10** treatment where we observed 10-fold higher expression of the target protein. Compounds **9** and **10** also induced expression of p-Akt, whereas compound **14** reduced its expression levels for 57 % in average compared to the untreated DHL-4 cells.

Interestingly, our results indicate opposing effects of compound **14** among ABC and GCB DLBCL cells on expression of two main targets, p-NF- $\kappa$ B and p-Akt. Treatment of DHL-4 cells with compound **14** showed reduction of p-Akt levels,

while in HBL-1 cells we observed increased expression of the target protein in average for 87 % compared to the control group. Compound **9** decreased expression of p-Akt in more aggressive DLBCL HBL-1 cells, while in DHL-4 cells we observed stimulated expression. Compound **10** elevated the expression of p-NF- $\kappa$ B and p-Akt in both cell lines (Figure 6), suggesting its stimulatory characteristics regarding the two key players in DLBCL tumorigenesis.

Constitutive activity of PI3K/Akt signaling as a core regulatory mechanism in many cancers is an important strategy for therapeutic approaches. However, cancer cells are characterized with an ability to adapt to drug-response signaling processes that lead to therapeutic resistance.<sup>[40,41]</sup> This is achieved through cell-to-cell cross-talk, feedback regulation, functional redundancies and many other mechanisms.<sup>[42]</sup> The activation of compensatory pathways is recognized as one of the limitations for therapeutic effectiveness. Serra *et al* have reported enhanced activity of ERK signaling after PI3K pathway inhibition in HER2-positive breast cancer.<sup>[43]</sup> In non-small cell lung cancer models, inhibition of PI3K signaling axis lead to enhanced activation of MET/STAT3 signaling pathway promoting cancer progression, metastasis and drug resistance.<sup>[44]</sup>

Although Akt activation promotes cell survival, different chemotherapeutic drugs stimulate Akt phosphorylation. This mechanism is commonly linked to chemoresistance of cancer cells. However, several reports suggest that activation of Akt by certain chemotherapies results in overall cellular therapeutic sensitivity.<sup>[45]</sup> In theory, each molecular target can be inhibited to improve the outcomes of conventional treatment. Therefore, multimodality treatment approach suggests the use of Akt inhibitors, such as MK-2206, perifosine and other inhibitors of PI3K/Akt signaling that induce sensitization of cancer cells to the therapy in *in vitro* and *in vivo* models.<sup>[46]</sup> Doxorubicin, paclitaxel, gemcitabine and 5-fluorouracil are chemotherapeutic drugs known to activate Akt phosphorylation in cancer models. This event potentially arises as a result of activation of cell defense mechanisms under certain stress or extracellular stimuli.<sup>[45,47]</sup> Several reports suggest that Akt activation is a main event linked with resistance to platinum-based therapy. Liu *et al* showed that induced expression of Akt1 is sufficient for induction of cell resistance to cisplatin therapy, while inhibition of Akt1 induced cisplatin sensitivity of lung cancer cells. In the same study, activation of Akt was highly correlated to cisplatin chemosensitivity in human tumor tissues obtained from lung cancer patients, suggesting Akt activation as a mechanism of drug resistance that could represent therapeutic target to avoid therapy resistance.<sup>[48]</sup> Accordingly, Akt inhibitor MK-2206 showed synergistic effect in combination with cisplatin in distinct tumors, such as lung, nasopharyngeal, gastric cancer and others, underlining the pivotal role of Akt activation in resistance to platinum drugs.<sup>[46]</sup>

Combinatorial treatments offer a promising approach in treatment of malignant models resistant to conventional therapy. Glamočlija *et al* (2022) recently reported synergistic effect of metformin and thymoquinone on decrease of cell viability and proliferation in imatinib-sensitive and imatinib-resistant leukemia cells, where the stronger effects of combinatorial treatment were observed in resistant compared to imatinib-sensitive cell models.<sup>[49]</sup> Therefore, implication of combinatorial therapy targeting diverse cellular mechanisms in cancer cells could offer a promising approach for cancer treatment in the future. Taking into consideration our findings and literature data, we can understand that proper combinatorial treatments with Akt inhibitors and conventional therapies could improve patient clinical benefits.

## CONCLUSION

In our study, compounds **9**, **10** and **14** influenced expression of PI3K $\delta$ , p-NF- $\kappa$ B and p-Akt in HBL-1 and DHL-4 cells, where mainly stimulatory activities were observed. ABC DLBCL cells showed greater sensitivity toward compound **9** in terms of p-Akt expression decrease, while GCB DLBCL cells exploited a greater sensitivity toward the treatment with compound **14**. Even though our results provide only an insight into activation of compensatory mechanism in DLBCL models upon treatment with xanthene derivatives, still it is important to underline that these data corroborate former findings and approaches for using dual inhibitors in cancer treatment for greater therapeutic effectiveness and therapeutic resistance escape.<sup>[44]</sup> We assume that the treatment would possibly result in even greater antitumor effectiveness if applied in combination with Akt inhibitors. This effect remains to be evaluated in the future.

**Supplementary Information.** Supporting information to the paper is attached to the electronic version of the article at: <https://doi.org/10.5562/cca4007>.

PDF files with attached documents are best viewed with Adobe Acrobat Reader which is free and can be downloaded from [Adobe's web site](https://www.adobe.com/acrobat).

## REFERENCES

- [1] H. Sung, J. Ferlay, R. L. Siegel, M. Laversanne, I. Soerjomataram, A. Jemal, F. Bray, *Ca-Cancer J. Clin.* **2021**, *71*, 209–249. <https://doi.org/10.3322/caac.21660>
- [2] R. Sever, J. S. Brugge, *Cold Spring Harbor Perspect. Med.* **2015**, *5*, 1–21. <https://doi.org/10.1101/cshperspect.a006098>
- [3] J. A. Engelman, *Nat. Rev. Cancer* **2009**, *9*, 550–562. <https://doi.org/10.1038/nrc2664>
- [4] Y. Peng, Y. Wang, C. Zhou, W. Mei, C. Zeng, *Front. Oncol.* **2022**, *12*, 819128. <https://doi.org/10.3389/fonc.2022.819128>
- [5] C. Porta, C. Paglino, A. Mosca, *Front. Oncol.* **2014**, *4*. <https://doi.org/10.3389/fonc.2014.00064>
- [6] E. Paplomata, R. T. O'Regan, *Ther. Adv. Med. Oncol.* **2014**, *6*, 154–166. <https://doi.org/10.1177/1758834014530023>
- [7] K. Taniguchi, M. Karin, *Nat. Rev. Immunol.* **2018**, *18*, 309–324. <https://doi.org/10.1038/nri.2017.142>
- [8] M. Jiang, N. N. Bennani, A. L. Feldman, *Expert Rev. Hematol.* **2017**, *10*, 405–415. <https://doi.org/10.1080/17474086.2017.1318053>
- [9] L. Wang, L. Li, K. H. Young, *J. Hematol. Oncol.* **2020**, *13*, 175. <https://doi.org/10.1186/s13045-020-01011-z>
- [10] J. Rovira, A. Valera, L. Colomo, X. Setoain, S. Rodríguez, A. Martínez-Trillos, E. Giné, I. Dlouhy, L. Magnano, A. Gaya, D. Martinez, E. Campo, A. Lopez-Guillermo, *Ann. Hematol.* **2015**, *94*, 803–812. <https://doi.org/10.1007/s00277-014-2271-1>
- [11] S. A. Padala, A. Kallam, *Diffuse Large B Cell Lymphoma* **2022**.
- [12] S. Li, K. H. Young, L. J. Medeiros, *Pathology* **2018**, *50*, 74–87. <https://doi.org/10.1016/j.pathol.2017.09.006>
- [13] L. H. Sehn, G. Salles, *N. Engl. J. Med.* **2021**, *384*, 842–858. <https://doi.org/10.1056/NEJMra2027612>
- [14] A. A. Alizadeh, M. B. Eisen, R. E. Davis, C. Ma, I. S. Lossos, A. Rosenwald, J. C. Boldrick, H. Sabet, T. Tran, X. Yu, J. I. Powell, L. Yang, G. E. Marti, T. Moore, J. Jr. Hudson, L. Lu, D. B. Lewis, R. Tibshirani, G. Sherlock, W. C. Chan, T. C. Greiner, D. D. Weisenburger, J. O. Armitage, R. Warnke, R. Levy, W. Wilson, R. G. Grever, J. C. Byrd, D. Botstein, P. O. Brown, L. M. Staudt, *Nature* **2000**, *403*, 503–511. <https://doi.org/10.1038/35000501>
- [15] G. Lenz, R. E. Davis, V. N. Ngo, L. Lam, T. C. George, G. W. Wright, S. S. Dave, H. Zhao, W. Xu, A. Rosenwald, G. Ott, H. K. Muller-Hermelink, R. D. Gascoyne, J. M. Connors, L. M. Rimsza, E. Campo, E. S. Jaffe, J. Delabie, E. B. Smeland, R. I. Fisher, W. C. Chan, L. M. Staudt, *Science* **2008**, *319*, 1676–1679. <https://doi.org/10.1126/science.1153629>
- [16] L. M. Staudt, *Cold Spring Harb. Perspect. Biol.* **2010**, *2*, a000109. <https://doi.org/10.1101/cshperspect.a000109>
- [17] K. Basso, U. Klein, H. Niu, G. A. Stolovitzky, Y. Tu, A. Califano, G. Cattoretti, R. Dalla-Favera, *Blood* **2004**, *104*, 4088–4096. <https://doi.org/10.1182/blood-2003-12-4291>



- [18] E. Veljović, S. Špirtović-Halilović, S. Muratović, A. Osmanović, S. Haverić, A. Haverić, M. Hadžić, M. Salihović, M. Malenica, A. Šapčanin, D. Završnik, *Acta Pharm.* **2019**, *69*, 683–694.  
<https://doi.org/10.2478/acph-2019-0044>
- [19] S. Zukić, E. Veljović, S. Špirtović-Halilović, S. Muratović, A. Osmanović, S. Trifunović, I. Novaković, D. Završnik, *Croat. Chem. Acta* **2018**, *91*, 1–9.  
<https://doi.org/10.5562/cca3225>
- [20] M. Maia, D. P. Resende, F. Durães, M. M. Pinto, E. Sousa, *Eur. J. Med. Chem.* **2021**, *210*, 113085.  
<https://doi.org/10.1016/j.ejmech.2020.113085>
- [21] H. Marona, N. Szkaradek, E. Karczewska, D. Trojanowska, A. Budak, P. Bober, W. Przepiórka, M. Cegla, E. Szneler, *Arch. Pharm. Chem. Life Sci.* **2009**, *342*, 9–18.  
<https://doi.org/10.1002/ardp.200800089>
- [22] K. M. Naidu, B. S. Krishna, M. A. Kumar, P. Arulselvan, S. I. Khalivulla, O. Lasekan, *Molecules* **2012**, *17*, 7543–7555.  
<https://doi.org/10.3390/molecules17067543>
- [23] H. N. Hafez, M. I. Hegab, I. S. Ahmed-Farag, A. B. A. el-Gazzar, *Bioorg. Med. Chem. Lett.* **2008**, *18*, 4538–4543.  
<https://doi.org/10.1016/j.bmcl.2008.07.042>
- [24] A. Seca, S. Leal, D. Pinto, M. Barreto, A. Silva, *Molecules* **2014**, *19*, 8317–8333.  
<https://doi.org/10.3390/molecules19068317>
- [25] B. C. Zorzanelli, L. N. de Queiroz, R. M. Santos, L. M. Menezes, F. C. Gomes, V. F. Ferreira, F. C. da Silva, B. K. Robbs, *Future Med. Chem.* **2018**, *10*, 1141.  
<https://doi.org/10.4155/fmc-2017-0205>
- [26] C. S. Bortolot, S. M. Forezi, R. F. Marra, M. P. Reis, B. E. Sá, R. I. Filho, Z. Ghasemishahrestani, M. Sola-Penna, P. Zancan, V. F. Ferreira, F. C. da Silva, *Med. Chem.* **2019**, *15*, 119–129.  
<https://doi.org/10.2174/1573406414666180524071409>
- [27] J. F. Thompson, S. S. Agarwala, B. M. Smithers, M. I. Ross, C. R. Scoggins, B. J. Coventry, S. J. Neuhaus, D. R. Minor, J. M. Singer, E.A. Wachter, *Ann. Surg. Oncol.* **2015**, *22*, 2135–2142.  
<https://doi.org/10.1245/s10434-014-4169-5>
- [28] E. Veljović, S. Špirtović-Halilović, S. Muratović, L. Valek Žulj, S. Roca, S. Trifunović, A. Osmanović, D. Završnik, *Croat. Chem. Acta* **2015**, *88*, 121–127.  
<https://doi.org/10.5562/cca2595>
- [29] L. Applova, E. Veljovic, S. Muratovic, J. Karlickova, K. Macakova, D. Završnik, L. Saso, K. Duric, P. Mladenka, *Med. Chem.* **2018**, *14*, 200–209.  
<https://doi.org/10.2174/1573406413666171010102535>
- [30] E. Krieger, G. Vriend, *J. Comput. Chem.* **2015**, *36*, 996–1007.  
<https://doi.org/10.1002/jcc.23899>
- [31] E. Krieger, G. Vriend, *Bioinformatics* **2014**, *30*, 2981–2982.  
<https://doi.org/10.1093/bioinformatics/btu426>
- [32] G. M. Morris, R. Huey, W. Lindstrom, M. F. Sanner, R. K. Belew, D. S. Goodsell, A. J. Olson, *J. Comput. Chem.* **2009**, *30*, 2785–2791.  
<https://doi.org/10.1002/jcc.21256>
- [33] Y. Duan, C. Wu, S. Chowdhury, M. C. Lee, G. Xiong, W. Zhang, R. Yang, P. Cieplak, R. Luo, T. Lee, J. Caldwell, J. Wang, P. Kollman, *J. Comput. Chem.* **2003**, *24*, 1999–2012.  
<https://doi.org/10.1002/jcc.10349>
- [34] D. M. Schnur, M. V. Grieshaber, J. P. Bowen, *J. Comput. Chem.* **1991**, *12*, 844–849.  
<https://doi.org/10.1002/jcc.540120709>
- [35] M. J. Dudek, J. W. Ponder, *J. Comput. Chem.* **1995**, *16*, 791–816.  
<https://doi.org/10.1002/jcc.540160702>
- [36] M. S. L. Kumar, J. Singh, S. K. Manna, S. Maji, R. Konwar, G. Panda, *Bioorg. Med. Chem. Lett.* **2018**, *4*, 778–782.  
<https://doi.org/10.1016/j.bmcl.2017.12.065>
- [37] A. G. Ghahsare, Z. S. Nazifi, S. M. R. Nazifi, *Curr. Org. Synth.* **2019**, *8*, 1071–1077.  
<https://doi.org/10.2174/1570179416666191017094908>
- [38] Y. Song, Y. Yang, L. Wu, N. Dong, S. Gao, H. Ji, X. Du, B. Liu, G. Chen, *Molecules* **2017**, *4*, 517.  
<https://doi.org/10.3390/molecules22040517>
- [39] S. K. Liew, S. Malagobadan, N. M. Arshad, N. H. Naqoor, *Biomolecules* **2020**, *1*, 138.  
<https://doi.org/10.3390/biom10010138>
- [40] J. S. Logue, D. K. Morrison, *Genes Dev.* **2012**, *26*, 641–650.  
<https://doi.org/10.1101/gad.186965.112>
- [41] L. Trusolino, A. Bertotti, *Cancer. Discov.* **2012**, *2*, 876–880.  
<https://doi.org/10.1158/2159-8290.CD-12-0400>
- [42] V. von Manstein, C. M. Yang, D. Richter, N. Delis, V. Vafaizadeh, B. Groner, *Curr. Signal Transduct. Ther.* **2013**, *8*, 193–202.  
<https://doi.org/10.2174/1574362409666140206221931>
- [43] S. Serra, A. Chicca, G. Delogu, S. Vázquez-Rodríguez, L. Santana, E. Uriarte, L. Casu, J. Gertsch, *Bioorg. Med. Chem. Lett.* **2012**, *22*, 5791–5794.  
<https://doi.org/10.1016/j.bmcl.2012.07.099>
- [44] C. Bian, Z. Liu, D. Li, L. P. Zhen, *Oncol. Lett.* **2018**, *15*, 9655.
- [45] X. Li, Y. Lu, K. Liang, B. Liu, Z. Fan, *Breast Cancer Res.* **2005**, *7*, R589.  
<https://doi.org/10.1186/bcr1259>
- [46] A. Avan, R. Narayan, E. Giovannetti, G. J. Peters, *World J. Clin. Oncol.* **2016**, *7*, 352–369.  
<https://doi.org/10.5306/wjco.v7.i5.352>

- [47] M. Alvarez-Tejado, S. Naranjo-Suárez, C. Jiménez, A. C. Carrera, M. O. Landázuri, L. del Peso, *J. Biol. Chem.* **2001**, *276*, 22368–22374. <https://doi.org/10.1074/jbc.M011688200>
- [48] L. Z. Liu, X. D. Zhou, G. Qian, X. Shi, J. Fang, B. H. Jiang, *Cancer Res.* **2007**, *67*, 6325–6332. <https://doi.org/10.1158/0008-5472.CAN-06-4261>
- [49] U. Glamoclija, L. Mahmutovic, E. Bilajac, V. Soljic, K. Vukojevic, M. Suljagic, *Front. Pharmacol.* **2022**, *13*, 867133. <https://doi.org/10.3389/fphar.2022.867133>